Electron energy distribution functions in low-pressure inductively coupled bounded plasmas

Albert Meige and Rod W. Boswell
Space Plasma, Power and Propulsion Group, Research School of Physical Sciences and Engineering, Australian National University, ACT 0200, Australia

(Received 5 June 2006; accepted 31 July 2006; published online 7 September 2006)

The electron energy distribution function (EEDF) in a low-pressure inductively coupled plasma confined between two infinite plates separated by 10 cm is investigated using a one-dimensional particle-in-cell simulation including Monte Carlo collisions. At low pressure, where the electron mean free path is of the order of or greater than the system length, the EEDF is close to Maxwellian, except for its tail, depleted at high energy. We give clear evidence that this depletion is mostly due to the high-energy electrons escaping to the walls. As a result of the EEDF nonlocality, the break energy, for which the depletion of the Maxwellian starts, is found to track the plasma potential. At a higher pressure, the electron mean free paths of the various elastic and inelastic collisions become shorter than the system length, resulting in a loss of nonlocality and the break energy of the distribution function moves to energies lower than the plasma potential. © *2006 American Institute of Physics*. [DOI: 10.1063/1.2339024]

I. INTRODUCTION

The form of the escaping electron energy distribution function (EEDF) has always been the subject of considerable discussion, as has the Maxwellianization of the electrons trapped between opposing sheaths. In capacitively coupled plasmas, two-temperature electron distribution functions are not rare and fall into two categories. (i) The first type, generally observed at some tens of mTorr, has a concave shape, presents a more energetic tail than the bulk Maxwellian distribution, and can be approximated as a sum of two Maxwellian distributions. Such bi-Maxwellian distributions in capacitive rf discharges are generally explained by the combination of the stochastic heating of the hot electrons at the rf electrode sheath and the trapping of the cold electrons by the ambipolar electric field, resulting in the existence of two distinct group of electrons. This was shown experimentally by Godyak and Piejak,[1] Godyak *et al.*,[2] and confirmed by subsequent experiments and particle-in-cell simulations by Turner *et al.*[3] (ii) The second type has a convex shape and is observed at a higher pressure, i.e., some hundreds of mTorr. In this case, the distribution function presents a drop or break in the slope, defining a sudden divergence away from the bulk Maxwellian distribution. The presence of this rapid drop for electron energies higher than a certain threshold is generally attributed to inelastic collisions.[4,5]

In inductively coupled plasmas (ICP), Godyak and Kolobov[6] measured even more complex distributions, having a three-temperature structure. Once again, the depletion at high energy, compared to Maxwellian, is, in general, attributed to inelastic collisions and, at lower pressure, to the escape of the fastest electrons, as it was shown by Granovski[7] and Godyak *et al.*[8]

In low-pressure discharges, below a few mTorr, collisions and especially inelastic collisions are rare and cannot alone explain the high-energy break in the EEDF. Biondi[9] already showed over 50 years ago that the loss to the walls might be responsible for the depleted tail of the distribution. He had identified this phenomenon, that he named "diffusive cooling," to be the main electron cooling mechanism in the afterglow of his "ionized gas." The effect of diffusive cooling has been previously studied, both theoretically and experimentally, in swarm physics[10–12] and plasma physics by a number of models.[13–15] In these studies, the loss of electrons to the walls was shown to be the main energy loss mechanism, but the assumption of Maxwellian distributions was made.

A more accurate kinetic approach was recently performed by Arslanbekov *et al.*,[16] Arslanbekov and Kudryavtsev,[17] where they showed that two main mechanisms exist for electron and energy loss: the first they called the "cutoff effect" and occurs when the trapped electrons become free electrons as the plasma potential collapses during the discharge afterglow. The second effect occurs when the trapped electrons gain energy through electron-electron collisions and are eventually pushed to energies higher than the plasma potential, thus becoming free electrons and escaping to the walls. Unlike the cutoff effect that occurs during the afterglow of a discharge, the second effect occurs even during the steady state. Kortshagen, Maresca and co-workers have experimentally shown some of Arslanbekov's results.[18,19] However, these experiments were only conducted in the afterglow regime of inductively coupled plasmas, i.e., in transitory regimes.

In the present paper, we use a particle-in-cell simulation to confirm the experimental measurements performed by Granovski[7] and Godyak *et al.*,[8] showing that at low pressure, the high-energy depletion of the EEDF is due to the fastest electrons escaping to the walls. It is shown that in steady-state plasmas, when the electron mean free path, and more precisely the energy relaxation length is of the order of or greater than the system length, electrons trapped in the well formed by the two sheaths at the boundaries have a Max-

wellian distribution, while the high energy tail of the EEDF is distinctly depleted. Clear evidence that the depletion at high energy of the EEDF is essentially due to the loss of the most energetic electrons to the walls is presented. The break energy, for which the depletion of the Maxwellian starts, occurs at the local plasma potential. That this break point tracks the plasma potential through the length of the simulation is due to the nonlocality of the electron distribution function.

II. MODEL

In the following, we wish to discuss the effect on the EEDF of the high-energy electrons lost to the walls. We do this by using a one-dimensional model in which an argon plasma is confined between two infinite plates separated by 10 cm. The neutral gas pressure is 1 mTorr and the steady-state electron density is 2×10^{15} m^{-3}. Our simulation is based on the well-known particle-in-cell (PIC) scheme[20–23] with Monte Carlo collisions (MCC),[24] including the three velocity dimensions. Accurate electron-neutral and ion-neutral collision cross sections are used to ensure realistic simulations; data can be found in Refs. 25 and 26 for electron-neutral collisions (elastic, exciting and ionizing), and in Ref. 27 for ion-neutral collisions (elastic and charge exchange). Coulomb collisions are not included in the present study, as their effect on the EEDF would be negligible under present conditions (low density).

One-dimensional PIC simulations are commonly concerned with capacitive coupling, where a rf voltage of some hundreds of volts is applied to one of the boundaries. This mechanism has been thoroughly studied[28–30] and creates a moving sheath that heats the electrons. The drawback of this process is that it leads to strongly affected plasma potentials and electron distributions. For the present investigation, the electrons are heated with a scheme intended to model "inductive" excitation, similar to that described by Turner,[31] but without solving electromagnetic field equations. Briefly, a rf electric field is applied in the y direction, perpendicular to the spatial dimension x of the PIC, which allows us to heat the electrons in the y direction, momentum and energy being transferred to the other x and z directions via electron-neutral collisions. In the following, the amplitude of the rf electric field is uniformly finite in the "source," i.e., the left half of the simulation and uniformly null in the diffusion chamber, i.e., the right half of the simulation. Some advantages of this scheme are that it avoids rf excursions of the potential in the plasma, characteristic of capacitive coupling, and it does not introduce any noticeable pathology in the electron transport.[32]

The simulations are allowed to run for several thousand rf cycles in order to reach a high degree of convergence. The number of macroparticles used is between 150 000 and 200 000, with 250 cells along the x axis and a time step of 5×10^{-11} s, which allows the simulation to meet the well-known stability and accuracy criteria of the PIC scheme.[20–23]

In the following, EEDFs are given in terms of normalized electron velocity distribution functions (EVDFs), resolved for the three different velocity components. They are measured along the abscissa with a spatial average over a distance of 0.4 mm and a temporal average over 100 rf cycles. The ordinate is log scale and a function of the electron energy, so that a Maxwellian distribution yields a straight line. To recapitulate, the simulated system has a finite size of 10 cm along the x direction, while it is infinite along the two other y and z directions, which allows the actual effect of the walls on the EEDFs to be determined. This is first done for a plasma sustaining an electric double layer and then for a simple inductively coupled plasma.

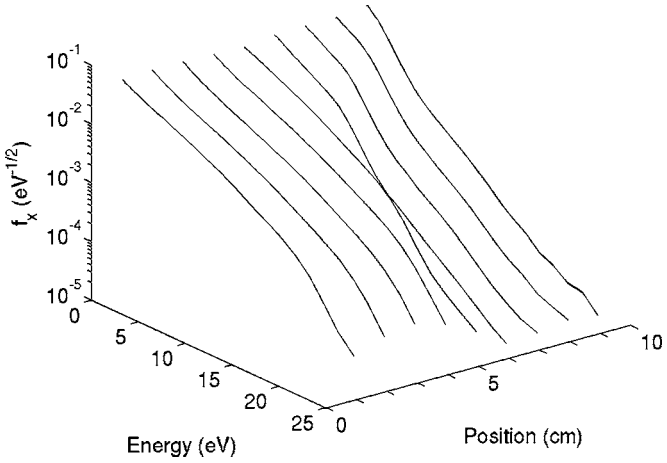

FIG. 1. x-velocity component of the EVDF f_x represented in log scale, as a function of the electron energy and at different positions in a double-layer plasma. The distributions are Maxwellian for the low-energy group of electrons and present a depleted tail at higher energy.

III. DOUBLE LAYER PLASMA

An electric double layer (DL) is a narrow localized region in a plasma that can sustain a large potential difference (Ref. 33 and references therein). Although DLs driven by currents (or imposed by potential differences) have been studied by computer simulation since the early 1970s,[34,35] the simulation described in Ref. 32 is, to our knowledge, the first numerical attempt to generate a current-free DL in an expanding plasma. An energy-independent particle loss process is introduced in the "diffusion chamber," to create a rapidly decreasing plasma density that can produce a spatially limited potential drop with the characteristics of a double layer. For these DL simulations, the left wall is allowed to float and the right wall is grounded. As the bulk plasma itself is supporting the 20 V double layer, this system presents an ideal opportunity to study the EEDF for different local plasma potentials.

Figure 1 shows the EVDF as a function of the electron energy at different positions in the plasma and it is quite clear that each of these distributions is Maxwellian at low energy, but presents a depleted tail at higher energy. The plasma potential profile along the system is shown as a solid line in Fig. 2 and about halfway across the system, i.e., at 5 cm where the loss process begins, the DL can be seen at the interface between the source and the diffusion chamber. Of particular relevance here is the following: the break energy $\mathcal{E}^*$ can be seen to depend on the position in the plasma

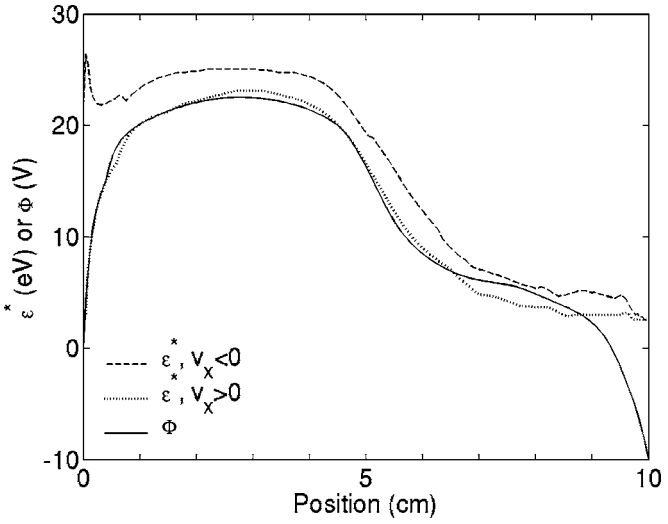

FIG. 2. Energy $\mathcal{E}^*$ of the EVDF break for positive (dotted line) and negative (dashed line) velocities as a function of position. The energy of the break tracks the plasma potential Φ of the double-layer plasma (solid line).

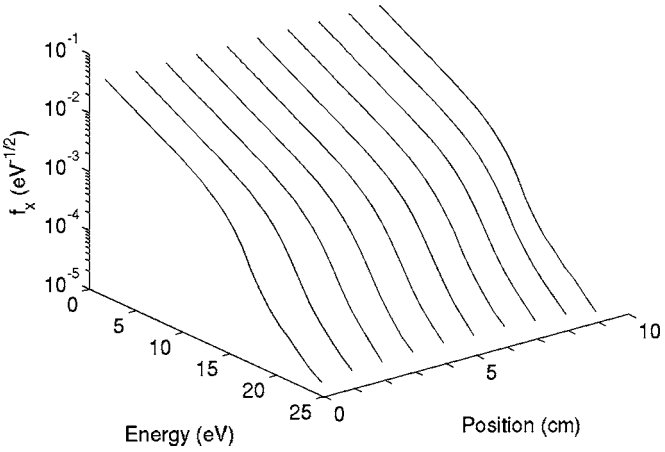

FIG. 3. x-velocity component of the EVDF f_x represented in log scale, as a function of the electron energy and at different positions in a simple inductively coupled plasma. The distributions are Maxwellian for the low-energy group of electrons and present a depleted tail at higher energy.

and tracks the local plasma potential. This is a direct consequence of the nonlocality of the electron distribution, where the EEDF is not in equilibrium with the local electric field.[36–38]

To make this point very clear, the dotted and dashed lines in Fig. 2 show the EVDF break energy, measured in eV, for both positive (right directed) and negative (left directed) electron velocities, respectively. For both cases, the energy corresponding to the break follows the local plasma potential. The EVDF break energy for negative velocities is found to occur at energies slightly higher than for positive velocities, presumably due to the asymmetry of the plasma potential profile and the potential difference between the left and right walls. When both walls are grounded a much less pronounced difference between the positive and negative velocities is observed.

IV. INDUCTIVELY COUPLED PLASMA

To check that the loss process that creates the double layer does not introduce nonphysical features in the EEDF, a simple inductively coupled plasma (ICP) is now investigated. The same parameters as in the previous section are used with the "inductive" heating mechanism on the left half of the system, but the particle loss process on the right half was deactivated. Figure 3 shows EVDFs across the plasma that are Maxwellian distributions with a depleted tail. Once again, as shown by Fig. 4, the EVDF break energy $\mathcal{E}^*$ tracks the plasma potential, but unlike the double-layer case, the break energy for the positive and negative velocities is the same. This tends to confirm that the difference between positive and negative velocities in the double-layer case was due to the highly nonsymmetrical nature of the system.

Hence, for both the double-layer plasma and the ICP, the presence of a sudden break in the EEDF for high-energy electrons was shown and due to the nonlocality of the EEDF, the energy of the break tracks the local plasma potential. As stated previously, at higher pressures, the break has been attributed to atomic processes arising from inelastic collisions, and at lower pressure to the high-energy electrons lost to the walls.

Figure 5 shows the EVDF in the bulk of the ICP for the three different velocity components and the spatially limited velocity direction of the EVDF f_x alone displays a break at high electron energies. The EVDF f_y and f_z corresponding to the perpendicular directions, i.e., where the plasma is not bounded, are almost Maxwellian, except for a very slight inflection, which is presumably due to rare inelastic collisions. If the significant break observed in f_x were also due to inelastic collisions, this would be clearly seen in the f_y and f_z components. In other words the substantial break observed in EVDF of the spatially limited direction appears to be mostly due to the loss of high-energy electrons to the walls.

As previously stated, the inductive heating mechanism acts in the perpendicular direction of the simulation and, at

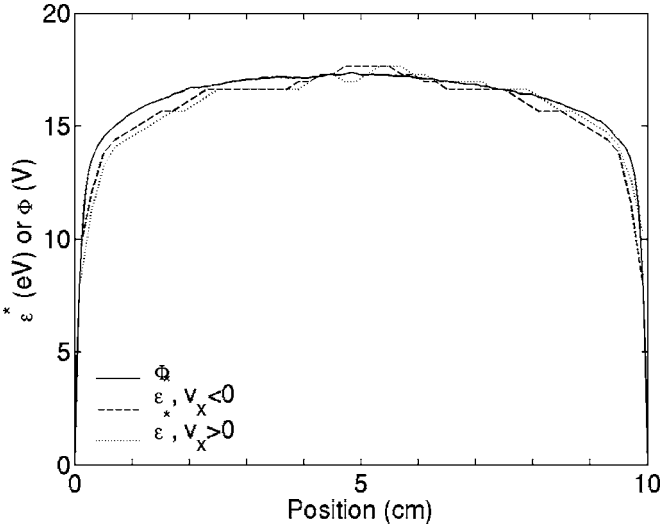

FIG. 4. Energy $\mathcal{E}^*$ of the EVDF break for positive (dotted line) and negative (dashed line) velocities as a function of position. The energy of the break tracks the plasma potential Φ of the simple inductively coupled plasma (solid line).

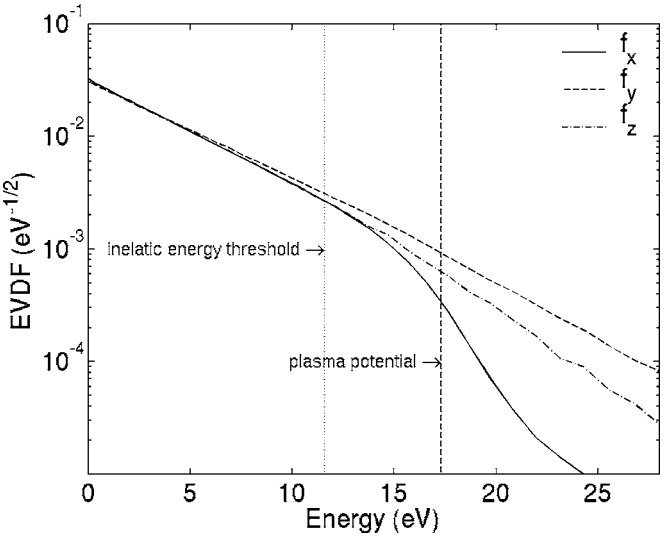

FIG. 5. Three velocity components of the EVDF measured in the bulk of the ICP and plotted as a function of electron energy. The distribution is depleted, compared to Maxwellian distribution, for the spatially limited velocity direction (f_x, solid line). On the other hand, EVDFs corresponding to the velocity direction for which the plasma is not bounded are Maxwellian (f_y and f_z, broken lines). The vertical dotted and dashed lines show the inelastic energy threshold and the local plasma potential, respectively.

low pressure, the energy relaxation rate is much longer than the momentum relaxation rate. Consequently, electrons suddenly acquiring enough momentum along x to be able to reach the walls after a single elastic collision have a high probability of actually escaping without undergoing another collision, and hence without being able to repopulate the tail of the distribution function. These electrons lost to the walls, i.e., the most energetic ones, remove a considerable amount of energy from the electron distribution function, hence depopulating the tail of the distribution.

For completeness, the numerical experiment was repeated for pressures between 0.1 to 100 mTorr. As expected from many experiments and glow discharge theory, the bulk electron temperature decreases when the pressure increases. Additionally, the EVDF break moves to lower energies, corresponding to the inelastic collision energy threshold, when increasing pressure. At low pressure, i.e., below a few mTorr, the plasma potential defines the limit of the Maxwellianization of the electrons, while at higher pressure the electron distribution appears to be governed by the shorter electron mean free path of the various elastic and inelastic processes.

V. DISCUSSION

The fact that the electron energy distribution functions presented above for both the double-layer plasmas and the ICP did not have any low-energy electron population was not considered until now. This appears to be in contradiction with the many experiments previously reported.[8]

At higher density, electron-electron Coulomb collisions are no longer negligible and would Maxwellianize the low-energy part of the distribution, and could explain the absence of low-energy population in the results presented above. However, under the conditions that were considered (low density), electron-electron Coulomb collisions are negligible and were not included in the model. To explain the absence of a low-energy peak in the distribution, we shall go back to its origin in real experimental systems. Low-energy electrons are trapped by the ambipolar electric field in the plasma bulk, thus they are prevented from participating in the heating process taking place in the skin layer. As stated previously, in the simulation the heating mechanism is located in the whole "source," i.e., in the whole left half of the simulation. Therefore, unlike in real inductively coupled plasma, there are no trapped electrons and all the electrons participate in the heating mechanism, which presumably explains the absence of low-energy population.

In addition, in the previous simulations, after an ionization event, the energy between the scattered and the created electron was chosen to be shared with a probability not depending on the energy of the incident electron, hence favoring the creation of relatively energetic electrons, which could presumably explain the absence of a cold population, even when the width of the heating region was reduced, to allow the existence of a nonheated trapped population of electrons.

To confirm this assumption, simulations where the heating region was as small as 0.5 cm, where a significant fraction of the electrons do not participate in the heating mechanism, were run with a different energy-sharing algorithm. Rather than equally sharing the energy between the scattered electron and the newly created electron after an ionization event, an energy-dependent mechanism, where the energy of the newly created electron is forced to be less than 1 eV was implemented. In this case a low-energy population of electrons was observed. However, this population of low-energy electrons is far from being as important as that experimentally measured and reported by Godyak *et al.*,[8] for example. It may well be that electrons in the elastic energy range suffer from numerical heating or that the simulations are simply not completely steady state, although run for thousands of rf cycles. This issue is currently being investigated by Legradic[39] both experimentally and by computer simulation.

VI. CONCLUSION

We have investigated inductively coupled plasmas (with and without an electric double layer) by the use of particle-in-cell simulation, including Monte Carlo collisions and a new "inductive" heating mechanism. We have shown that when the electron energy relaxation length is greater than the system dimension, electrons lost to the walls are the main mechanism for the high-energy depletion of the EEDF. These results confirm earlier experimental results by Granovski[7] and Godyak *et al.*[8]

[1] V. A. Godyak and R. B. Piejak, Phys. Rev. Lett. **65**, 996 (1990).
[2] V. A. Godyak, R. B. Piejak, and B. M. Alexandrovich, Phys. Rev. Lett. **68**, 40 (1992).
[3] M. M. Turner, R. A. Doyle, and M. B. Hopkins, Appl. Phys. Lett. **62**, 3247 (1993).
[4] V. A. Godyak and R. B. Piejak, Appl. Phys. Lett. **63**, 3137 (1993).
[5] V. A. Godyak, V. P. Meytlis, and H. R. Strauss, IEEE Trans. Plasma Sci. **23**, 728 (1995).
[6] V. A. Godyak and V. I. Kolobov, Phys. Rev. Lett. **81**, 369 (1998).
[7] L. Granovski, *Electric Current in Gas (Steady Current)* (Nauka, Moscow, 1971).

[8] V. A. Godyak, R. B. Piejak, and B. M. Alexandrovich, Plasma Sources Sci. Technol. **11**, 525 (2002).
[9] M. A. Biondi, Phys. Rev. **93**, 1136 (1954).
[10] R. E. Robson, Phys. Rev. E **61**, 848 (2000).
[11] J. H. Parker, Phys. Rev. **139**, 1792 (1965).
[12] T. Rhymes and R. W. Crompton, Aust. J. Phys. **28**, 675 (1975).
[13] S. Ashida, C. Lee, and M. A. Lieberman, J. Vac. Sci. Technol. A **13**, 2498 (1995).
[14] S. Ashida, M. R. Shim, and M. A. Lieberman, J. Vac. Sci. Technol. A **14**, 391 (1996).
[15] V. I. Kolobov, D. P. Lymberopoulos, and D. J. Economou, Phys. Rev. E **55**, 3408 (1997).
[16] R. R. Arslanbekov, A. A. Kudryavtsev, and L. D. Tsendin, Phys. Rev. E **64**, 016401 (2001).
[17] R. R. Arslanbekov and A. A. Kudryavtsev, Phys. Rev. E **58**, 7785 (1998).
[18] U. Kortshagen, A. Maresca, K. Korlov, and B. Heil, Appl. Surf. Sci. **192**, 244 (2002).
[19] A. Maresca, K. Orlov, and U. Kortshagen, Phys. Rev. E **65**, 056405 (2002).
[20] C. K. Birdsall and D. Fuss, J. Comput. Phys. **3**, 494 (1969).
[21] A. B. Langdon and C. K. Birdsall, Phys. Fluids **13**, 2115 (1970).
[22] R. W. Hockney and J. W. Eastwood, *Computer Simulation Using Particles* (IOP, Bristol, 1988).
[23] C. K. Birdsall and A. B. Langdon, *Plasma Physics Via Computer Simulation* (IOP, Bristol, 1991).
[24] V. Vahedi and M. Surendra, Comput. Phys. Commun. **87**, 179 (1995).
[25] K. Tachibana, Phys. Rev. A **34**, 1007 (1986).
[26] J. L. Pack, R. E. Voshall, A. V. Phelps, and L. E. Kline, J. Appl. Phys. **71**, 5363 (1992).
[27] A. V. Phelps, J. Appl. Phys. **1994**, 747 (1994).
[28] D. Vender, Ph.D. thesis, Research School of Physical Science and Engineering—Australian National University, 1990.
[29] D. Vender and R. W. Boswell, IEEE Trans. Plasma Sci. **18**, 725 (1990).
[30] M. A. Lieberman and A. J. Lichtenberg, *Principles of Plasma Discharges and Materials Processing* (Wiley Interscience, New York, 1994).
[31] M. M. Turner, Phys. Rev. Lett. **71**, 1844 (1993).
[32] A. Meige, R. W. Boswell, C. Charles, and M. M. Turner, Phys. Plasmas **12**, 052317 (2005).
[33] M. A. Raadu, Phys. Rep. **178**, 25 (1989).
[34] C. K. Goertz and G. Joyce, Astrophys. Space Sci. **32**, 165 (1975).
[35] G. Joyce and R. F. Hubbard, J. Plasma Phys. **20**, 391 (1978).
[36] I. B. Bernstein and T. Holstein, Phys. Rev. **94**, 1475 (1954).
[37] L. D. Tsendin, Sov. Phys. JETP **39**, 805 (1974).
[38] V. I. Kolobov and V. A. Godyak, IEEE Trans. Plasma Sci. **23**, 503 (1995).
[39] B. Legradic, Master's thesis, Space Plasma, Power and Propulsion—The Australian National University, 2006.